



Hydrogen sorption in Pd monolayers in alkaline solution

M.H. Martin, A. Lasia*

Département de chimie, Université de Sherbrooke, 2500 Blvd. de l'Université, Sherbrooke, Québec, Canada, J1K 2R1

ARTICLE INFO

Article history:

Received 29 October 2008

Received in revised form 7 January 2009

Accepted 16 January 2009

Available online 24 January 2009

Keywords:

Hydrogen adsorption and absorption

Palladium monolayers

Alkaline solutions

Benzotriazole

Isotherms

Impedance spectroscopy

ABSTRACT

Hydrogen adsorption/absorption at palladium monolayers (ML) deposited on monocrystalline Au(111) electrode was studied in 0.1 M NaOH solution. H charge isotherms demonstrated that adsorption started at potentials more positive than at thicker nanometric Pd/Au(polycrystal) deposits. Due to 3-dimensional deposit growth, absorption could be seen at all deposits thicker than 1 ML. Besides, H sorption at Pd/Au(111) monolayers was more reversible than at nanometric Pd/Au(polycrystal) deposits. Strong geometric and electronic effects due to the Au substrate were observed up to 5 Pd ML. Influence of benzotriazole (BTA) on H sorption was also investigated. BTA blocked H adsorption above 250 mV vs. RHE. At less positive potentials adsorbed BTA layer seemed to undergo a reorientation allowing H adsorption. Stationary and dynamic electrochemical impedance spectroscopy was used to obtain double layer capacitance and charge transfer resistance. BTA also promoted kinetically H sorption into Pd/Au(111) monolayer and Pd/Au(polycrystal) nanometric deposits.

© 2009 Elsevier Ltd. All rights reserved.

1. Introduction

Palladium has been intensively investigated, mainly because of its capacity to adsorb and absorb large amount of hydrogen [1,2]. Besides, Pd is also used for its catalytic properties. Since it is an expensive material, the interest of using it as thin films is obvious. Moreover, deposits in the monolayer range exhibit different catalytic properties due to the interactions between the substrate and the deposit [3,4]. Czerwinski et al. studied H sorption into Pd thin films in both acid and alkaline media [5–12]. Following their work, nanometric Pd films deposited at polycrystalline gold electrode were studied by our group in acid media [13–17] and in NaOH [18]. Paillier and Roué [19] also investigated H sorption at Pd/Au(polycrystal) nanometric films in KOH. In parallel, Pd monolayers deposited on monocrystals demonstrated interesting properties. The first studies of Pd deposition on Pt(111) were carried out by Clavilier et al. [20] and Attard and Bannister [21]. Kolb and coworkers have also investigated Pd deposition on Au [22–25], Pt [26,27], Rh [28] and other monocrystals [27] exploring the influence of anions during deposition and showing that the Pd growth was 3-dimensional after the first monolayer. In our earlier papers deposits on monocrystals Pd/Au(111) and Pt(111) were studied to better understand adsorption and absorption mechanisms in sulfuric and perchloric acid, determine H isotherms and using impedance measurements to evaluate kinetic effects [13,15,16,29,30]. However, until now no studies were carried out in alkaline media.

Another interesting way to get a better understanding of adsorption and absorption mechanisms is to use a poison that will block one of the two hydrogen sorption reactions. Conway et al. [31,32] investigated the influence of As on H insertion into Fe and steel in alkaline media and found that the coverage ratio of metal by adsorbed hydrogen is decreased but, at very negative potentials, H absorption is promoted. Birry [33] studied influence of As on H sorption into Pd and found very strong poisoning effect even at very low As concentrations but the results were not reproducible. The role of thiourea was also studied [31,34] and a similar poisoning behavior was observed. Carbon monoxide is also known for poisoning Pd surfaces and blocking adsorption and absorption [35–40]. More recently, our group looked at the effect of crystal violet on H sorption at Pd thin films in acidic solutions [13,29], following a preliminary work of Baldauf and Kolb [22]. It was concluded that crystal violet inhibits H adsorption and makes absorption more reversible, which was confirmed by observations of Bartlett et al. [41,42]. However, crystal violet is insoluble in alkaline solutions. Another interesting molecule to study H sorption in alkaline media is benzotriazole (BTA). It is widely used and studied for its anti-corrosion protective ability. Baldauf and Kolb [22] also demonstrated that BTA could have poisoning properties towards H sorption into Pd even in acid media. Elhamid et al. [43] and Amokrane et al. [44] showed that BTA blocks H adsorption at Fe and diminish H permeation. To the best of our knowledge, no further investigations on the influence of BTA on H sorption in Pd thin films have been carried out.

In the present work cyclic voltammetry, H charge isotherms and impedance spectroscopy were used to study nanometric palladium films on Au(polycrystal) and Pd/Au(111) monolayers, in 0.1 M NaOH, with and without addition of benzotriazole.

* Corresponding author. Tel.: +1 819 821 7097; fax: +1 819 821 8017.
E-mail address: a.lasia@usherbrooke.ca (A. Lasia).

2. Experimental

The 30 and 70 nm palladium films were deposited on a polycrystalline gold electrode, with a surface area of 0.322 cm^2 , from a bath containing 0.1 M PdCl_2 (Aldrich, 99%) + 0.3 M LiCl (Aldrich, 99%), at a current density of 1 mA cm^{-2} [13,45].

Au(111) monocrystalline electrode had a geometric surface area of 0.332 cm^2 and was prepared by Morin and Langlois from University of Ottawa, following the method described earlier [46,47]. Pd monolayers were deposited on this gold monocrystal, from a bath containing $0.1 \text{ M H}_2\text{SO}_4$ (Seastar Baseline) and $1 \text{ mM K}_2\text{PdCl}_4$ (Aldrich, 99.99%), by scanning electrode potential at 0.1 mV s^{-1} from 0.931 to 0.841 V vs. reversible hydrogen electrode (RHE), following the protocol of Duncan and Lasia [29]. The apparent number of monolayers was estimated from the deposition charge, assuming that $440 \mu\text{C cm}^{-2}$ is needed to form a Pd monolayer on Au(111) monocrystal [22].

The measurements were carried out in 0.1 M NaOH (Aldrich, 99.998%), and $0.1 \text{ M NaOH} + 10 \text{ mM BTA}$ (Aldrich, 99%). All solutions were prepared using nanopure water (Millipore, Milli-Q gradient system) and deoxygenated by bubbling argon (Praxair, Ar UHP 5.0).

A platinum gauze and an Hg | HgO in 0.1 M NaOH were used as counter and reference electrode, respectively. The reference electrode potential was $E = +935 \text{ mV}$ vs. reversible hydrogen electrode RHE in the same solution. All the potentials are reported vs. RHE in the same solution. The working electrode was used in a hanging meniscus configuration.

To get more reproducible results taking into account quite fast surface contamination in alkaline solution (contrary to the acid solutions), before and after short series of experiments, the electrode was transferred into $0.1 \text{ M H}_2\text{SO}_4$ and cycled between $+100$ and $+500 \text{ mV}$ at 50 mV s^{-1} until a correct [13,14] voltammogram was obtained, after which the experiment was continued in alkaline solution. Repeating such a procedure regularly allowed for obtaining of reproducible results. The treatment in H_2SO_4 consisted of series of cyclic voltammograms in the same potential range at 50 mV s^{-1} and polarizations at $+100 \text{ mV}$ during 30 s .

The electrochemical measurements were carried out using a Solartron SI 1260 Frequency Response Analyzer, and a Princeton Applied Research 273A potentiostat. The Dynamic Electrochemical Impedance Spectroscopy (DEIS) was used by applying a sum of 35 odd harmonic frequencies during the potential sweep through PAR 273A potentiostat. The generation of the ac signal as well as the data acquisition was carried out using Keithley KSUB3116 D/A and A/D module. The electronics for the signal amplification/attenuation and subtraction/addition was carried out using a homemade electronic system. The amplitude of the ac signals was varied with frequency according to the suggestion of Popkurov and Schindler [48] and the phases were randomized. The data generation, acquisition, and analysis program was written and provided by D. Harrington, University of Victoria.

3. Results and discussion

3.1. H sorption at Pd monolayers

Fig. 1 displays the voltammograms at a 70 nm Pd film deposited on a polycrystalline Au and 10 monolayers (ML) Pd deposited on Au(111) electrodes. A detailed description of voltammograms for nanometric Pd films (tenths of nanometers thickness) was already given in our previous work [18]. Five different peaks can be distinguished at Pd monolayers. Considering earlier works [18,49,50] and the potential range at which they appear A_1 and C_1 were attributed to H adsorption and desorption. Peaks A_2 , A_3 and C_2 were attributed to H adsorption and desorption. Two anodic peaks were already seen at nanometric Pd films (see peaks A_1 and A_1' in [18] or A_2

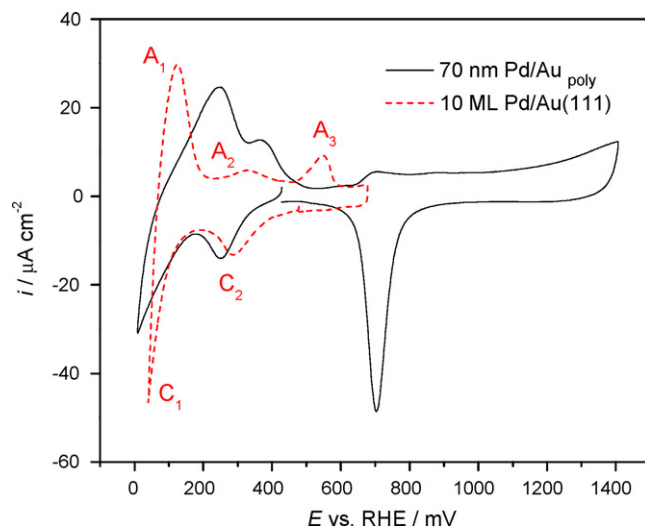


Fig. 1. Cyclic voltammograms at a 70 nm Pd deposit (—) and $10 \text{ ML Pd/Au}(111)$ deposit (---), in 0.1 M NaOH ; scan rate: 10 mV s^{-1} .

and A_2' in Ref. [50]). The presence of two different sites at the Pd surface could be the reason for this phenomenon. Two peaks were also observed in H_2SO_4 at Pd/Au(111) thin deposits until 10 monolayers [22,29]. The peak at more positive potentials was related to hydrogen adsorption at the steps while the second peak was representative of adsorption on terraces.

Comparison between the voltammograms at a 10 ML Pd deposit and a 70 nm Pd film shows that adsorption at Pd monolayer deposits begins at more positive potentials. Similar behavior was observed in acid solutions [14,29]. The second observation is an important increase of the reversibility of the H-absorption reaction at Pd monolayers (peaks C_1 and A_1) in comparison with nanometric Pd films. This kinetic effect could be a consequence of the substrate influence. This was confirmed by the impedance measurements.

Fig. 2 allows for a better understanding of the nature of different peaks, as well as for the effect of the electrode surface contamination. The electrode was cycled in alkaline solution after pretreatment in $0.1 \text{ M H}_2\text{SO}_4$, see Section 2 for details. Since the deposit was perfectly stable (reproducible cyclic voltammograms) in sulfuric acid, the evolution in voltammograms recorded in 0.1 M NaOH and displayed in Fig. 2 could not be due to changes in

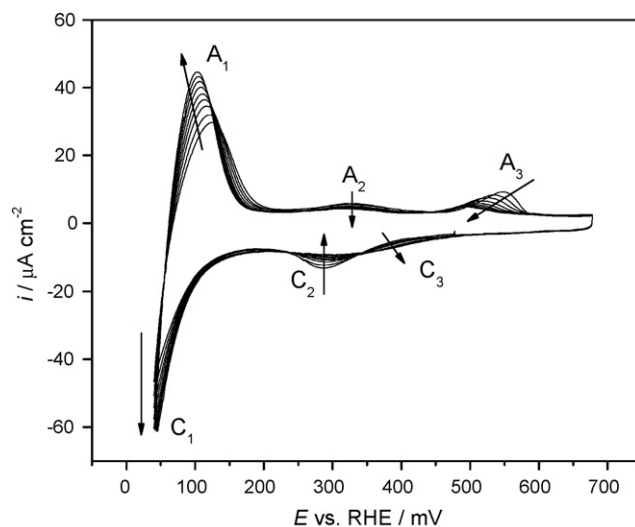


Fig. 2. Evolution of cyclic voltammograms with the number of cycles, at a $10 \text{ ML Pd/Au}(111)$ film; scan rate: 10 mV s^{-1} .

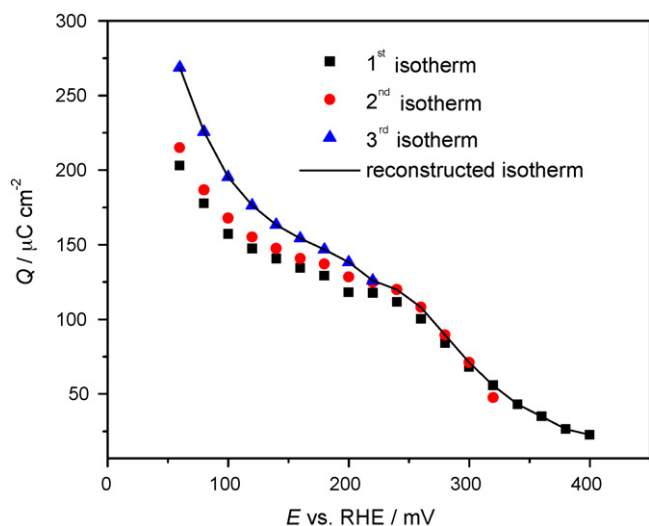


Fig. 3. Successively measured isotherms at a 7 ML Pd/Au(1 1 1) deposit, 1st isotherm (■) between 420 and 60 mV, 2nd isotherm (●) between 320 and 60 mV, 3rd isotherm (▲) between 220 and 60 mV, and the final isotherm reconstructed from the three series (in continuous line).

the deposit's morphology. Focusing on the peaks at more positive potentials (C_3 , C_2 , A_3 and A_2), it is obvious that they decrease with the number of cycles, with the exception of C_3 , which is increasing. Therefore, as the hydrogen adsorption seems to be blocked peak C_3 cannot be ascribed to the adsorption process. We therefore considered the hypothesis of surface contamination by traces impurities present in alkaline solution, and referred C_3 to a contaminant adsorption. This contamination seems to act as an adsorption blocker and an absorption promoter, i.e. the same effect as that of BTA (see below) or crystal violet [13,29].

Fig. 3 is an example of the surface contamination illustrated in the case of determination of the H sorption isotherms at 7 ML Pd/Au(1 1 1). The first isotherm determination was carried out after the same pretreatment in H_2SO_4 described in the last paragraph. After the deposit was considered as stable in acid, i.e. there were no changes in the voltammograms and results were similar to those in the literature [13,14], it was transferred into NaOH, and the measurements were carried out in the following way: polarization at 420 mV during 30 s, electrochemical impedance spectroscopy (EIS) measurements from 20 kHz to 20 mHz, discharge at 650 mV (in the non-faradaic potential zone), cyclic voltammetry at 200 mV s^{-1} , polarization at 400 mV during 30 s, and so on every 20 mV until $E = 60\text{ mV}$. These experiments took around 2 h 30 min. Similar series of experiments but without impedance measurements gave reproducible results, in a shorter experiment time (around 40 min). The first setup with full impedance measurements gave non-reproducible results with isotherms systematically lower than what was obtained during the experiments without impedance measurements. The fact that longer polarization times due to impedance measurements seemed to drastically decrease the H sorption charge confirmed again the hypothesis of surface contamination. Our first idea to counter this problem was to decrease the frequency range to reduce the duration of our experiments. However, this was not sufficient to obtain reproducible results. Because the problem of contamination does not exist in acid media, we tried to "clean" our surface in acid solution after the first isotherm by carrying out the same pretreatment as before in H_2SO_4 . After 3 cyclic voltammetric polarization sweeps in H_2SO_4 the same cyclic voltammetric profile as that obtained during the first pretreatment and the same H sorption charge at 100 mV were found. Following this reactivation step, the Pd deposit was transferred back into NaOH and the same polarization/impedance/discharge/voltammetry setup was carried

out. However, we began our experiment from 320 mV instead of 420 mV. We finally carried out 3rd isotherm measurements in the potential range of 220 and 60 mV, after another cleaning in H_2SO_4 . Fig. 3 clearly shows that the 3rd isotherm is higher than the 2nd isotherm, which is higher than the 1st one. The final isotherm reported for H sorption at a 7 ML Pd deposit is thus the maximal isotherm, i.e. the 1st one between 420 and 320 mV, the 2nd between 320 and 240 mV, and the third one between 220 and 60 mV. This setup gave us reproducible results, with clear thickness dependence of the H oxidation charge. Moreover, these results were similar to those obtained when carrying out very short experiments without impedance measurements. Ideally, a cleaning would be performed after each measurement (polarization/impedance/discharge) at a single potential in NaOH. However, each opening of the electrochemical glass cell and transfer of the electrode increased the risk of important contamination. Therefore, we considered that our setup was the best compromise in our "race" against contamination.

Isotherms at Pd thin deposits with thicknesses between 1 and 10 ML are presented in Fig. 4, including the adsorption charge density Q_{ads} obtained earlier [18] at thicker Pd/Au(polycrystal) deposits by separations of adsorption and absorption contributions from the regression analysis. As mentioned in our earlier works [13,29], it is practically impossible to electro-deposit more than 0.8 ML Pd on Au(1 1 1) as the first monolayer. Therefore, the isotherm for 0.8 ML was normalized, considering that only 80% of the Au electrode surface was covered by Pd. Since there was obviously no absorption at 0.8 ML and just adsorption, isotherm at this thickness can directly be compared with the adsorption isotherm at nanometric Pd/Au(polycrystal) films. This comparison confirms what was observed in cyclic voltammetry, i.e. adsorption starts at more positive potentials at Pd/Au(1 1 1) monolayer deposits. This is because the first monolayers have different properties than bulk Pd. The substrate has multiple effects on H adsorption and absorption in Pd. First, as the Pd deposition on gold is pseudomorphic [25], Pd deposits have the same orientation as gold electrode, i.e. (1 1 1). It has been demonstrated that specific crystallographic orientation could strongly modify the electrochemical behavior of electrodes [27]. Moreover, the interatomic distances at the first layer are different. The interatomic distances in bulk Pd(1 1 1) is 2.75 Å while they are 2.88 Å for Pd on Au(1 1 1) [51]. Therefore, stress appears in the first Pd layers. These two phenomena can be grouped as the geometric effect of the substrate. Moreover, Sellidj and Koel [52] showed that the work function of Pd monolayers deposited on Au(1 1 1) is influenced by the substrate up to 5 monolayers. Fermi level is also

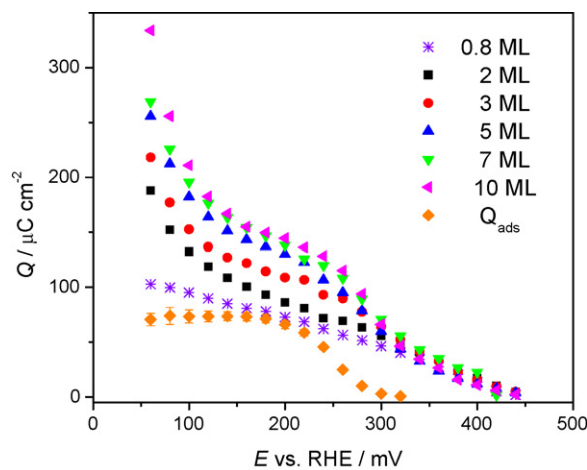


Fig. 4. Total H sorption isotherms at 0.8 ML (*), 2 ML (■), 3 ML (●), 5 ML (▲), 7 ML (▼) and 10 ML (◆) Pd/Au(1 1 1) deposits, and H adsorption charge density (◆) at Pd/Au(polycrystal).

modified [27,53,54]. These electronic effects can drastically modify adsorption properties of Pd deposits. Of course these two effects are interrelated.

The fact that isotherms are independent of thickness at potentials above 320 mV demonstrates that adsorption is predominant in this range of potentials while the absorption is practically inexistent. Below 320 mV, absorption becomes a significant part of the total H charge as it increases with the thickness. Below 120 mV, the charge strongly increases for all deposits except 0.8 ML. This phenomenon appears at potentials still too high to be related to H evolution, therefore, it must be attributed to absorption. This is in agreement with the fact that such a behavior was not visible at 0.8 ML. However, the increase below 120 mV at 2 ML is almost as strong as for thicker deposits, even if Baldauf and Kolb [22] demonstrated that at least 3 monolayers are normally required for absorption. This confirms the hypothesis of a 3-dimensional growth during deposition, i.e. the third layer (and higher) starts to be formed before the completion of the second layer [22,55]. Fig. 4 also clearly shows that the increase in the H charge with the thickness between 0.8 and 5 ML is much more important than between 5 and 10 ML. This is probably due to the substrate influence, which becomes less and less important with the increase in the Pd layer thickness.

Electrochemical impedance spectroscopy was also used to study Pd monolayers using the setup described above, i.e. a first sequence from 420 to 60 mV, cleaning in H₂SO₄, new sequence in NaOH from 320 to 60 mV, cleaning in H₂SO₄, and the last series of measurements from 220 to 60 mV in NaOH. As for the isotherms measurements, the impedance parameters were reconstructed from these three sequences. Due to the multiple electrode treatments in different electrolytes and the poor stability of 0.8 ML Pd/Au(1 1 1) deposit, no reliable impedance results could be obtained for this thickness.

Because very short experimental times were required to counter the electrode contamination and to obtain reproducible results, our frequency range was limited to 20 kHz–2 Hz with five points per decade. Fig. 5 shows examples of complex plane plots for H sorption at 7 ML Pd/Au(1 1 1) deposit, at four different potentials, with their complex nonlinear least-squares fits. The equivalent circuit used to fit our results was derived from the one presented in our earlier works [13,14,18,29] and consisted of a solution resistance in series with a double layer capacitance, which is in parallel with the charge transfer resistance-low frequency capacitance connection in

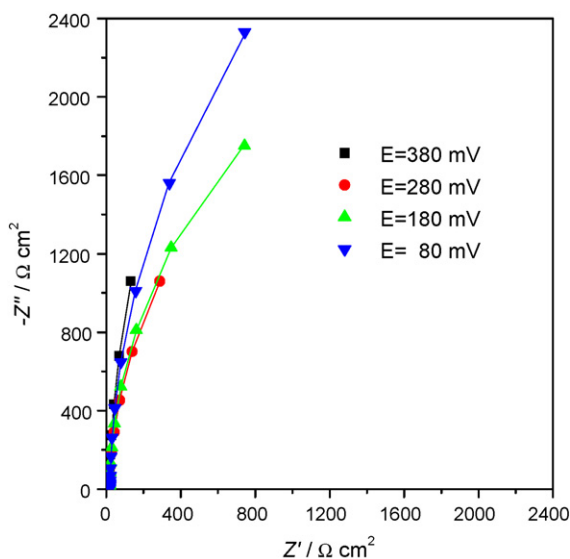


Fig. 5. Experimental complex plane plots (dot) and fitting (line) at a 7 monolayers Pd/Au(1 1 1) deposit, at four different potentials.

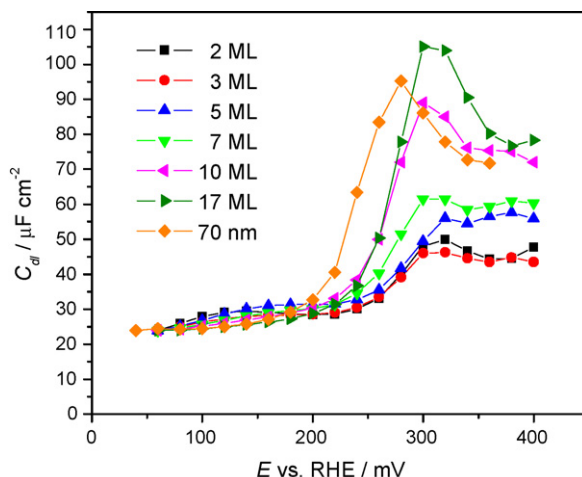


Fig. 6. Double layer capacitance, C_{dl} , at 2–17 ML Pd/Au(1 1 1) and 70 nm Pd/Au(polycrystal) in 0.1 M NaOH.

series. However, because our experiments were limited to higher frequencies, the complex plane plots only exhibited the beginning of the semi-circle, and the capacitive wall normally observed in the range of 0.1–0.01 Hz was never visible. Thus, the equivalent circuit used to fit our results was just a solution resistance R_s in series with a two branches circuit composed by the double layer capacitance C_{dl} in parallel with the charge transfer resistance R_{ct} . To take into account the non-homogeneity of the double layer capacitance, a constant phase element (CPE) was used for the double layer capacitance [56,57]. The average value of the capacitance was estimated from the parameters T and ϕ using equation [56]:

$$\bar{C}_{dl} = T^{1/\phi} \left(\frac{1}{R_s} + \frac{1}{R_{ct}} \right)^{1-1/\phi}$$

Fitting data to this model gave us maximal standard deviation of 1.5% for R_{ct} for potentials above 340 mV, and around 0.7% for potentials between 340 and 60 mV. This error is acceptable taking into account sensitivity of this parameter to contamination.

The potential dependence of the double layer capacitance C_{dl} for 70 nm Pd/Au(polycrystal) and Pd/Au(1 1 1) monolayer deposits is displayed in Fig. 6. At monolayer deposits, the values of C_{dl} in the potential range between 260 and 400 mV seem to depend on the deposit thickness. Potential dependence of C_{dl} at 10 and 17 ML Pd/Au(1 1 1) deposits are quite similar to that at 70 nm Pd/Au(polycrystal), with a shift of 20 mV. For nanometric Pd/Au(polycrystal) deposits, C_{dl} curves were similar at all thickness between 10 and 90 nm. This evolution in the C_{dl} potential dependence could be a consequence of the substrate effect. It has also been noticed that the substrate greatly influenced sulfate adsorption at Pd in H₂SO₄ [30]. The same phenomenon seems to exist in NaOH with OH adsorption.

Fig. 7 shows the potential dependence of the charge transfer resistance, R_{ct} , for Pd/Au(1 1 1) deposits, with thicknesses between 2 and 17 ML. For comparison, R_{ct} at 70 nm Pd/Au(polycrystal) is also displayed. Fig. 7 confirms that H adsorption is faster at Pd/Au(1 1 1) monolayers. Indeed, depending on the thickness, R_{ct} is between 2 and 8 times lower at Pd/Au(1 1 1) monolayers.

The isotherms in Fig. 4 showed that H absorption appears for all deposits thicker than 1 ML due to 3-dimensional growth. The simulations published earlier [29] and the experimental results demonstrate that $\log R_{ct}$ vs. potential curves should have a W-shape when adsorption and absorption processes coexist, with kinetic parameters of the same order of magnitude [18,29]. In the case when one of these reactions is much faster than the other, $\log R_{ct}$ vs. potential curves exhibit a single V-shape related to the fastest

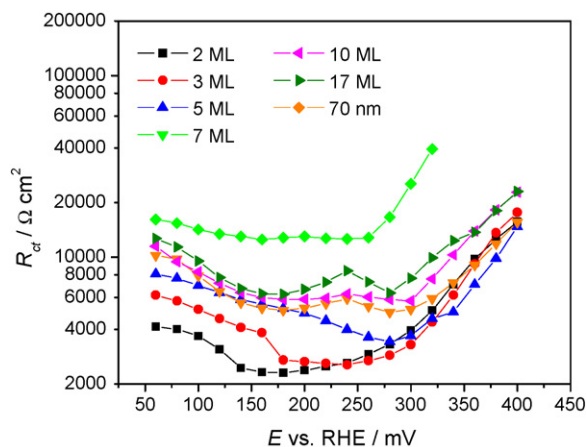


Fig. 7. Charge transfer resistance R_{ct} at 2–17 ML Pd/Au(111) in 0.1 M NaOH.

reaction, since adsorption and direct absorption reactions compete in parallel. Focusing on 2, 3 and 5 monolayers, a single V-shape attributed to H adsorption process is observed. Thus, it can be concluded that adsorption at Pd/Au(111) deposits thinner than 5 ML is faster than absorption between 400 and 60 mV. The fact that a surface property (R_{ct} of adsorption reaction) is thickness dependent strongly suggests that the kinetic promotion of adsorption is caused by the substrate effect. For thicker deposits, the W-shape is clearly visible. The rates of adsorption and absorption are of the same order of magnitude. Moreover, the evolution of the shape of R_{ct} vs. E with thickness leads to the conclusion that the kinetic promotion of adsorption for deposits thinner than 5 ML is strongly linked to the effects of the substrate. We have already demonstrated that the substrate effects can also strongly interfere with the thickness dependence of R_{ct} . While R_{ct} decreases with thickness at Pd/Au(111) monolayer deposits in H_2SO_4 [29], it increases at Pd/Pt(111) deposits [30]. In NaOH R_{ct} increases with thickness at Pd/Au(111) nanolayers while it decreases at nanometric Pd/Au(polycrystal) deposits [18].

3.2. Influence of the BTA on the H sorption in Pd

Fig. 8 presents the voltammograms for 70 nm Pd/Au(polycrystal) and 7 ML Pd/Au(111) deposits in 0.1 M NaOH, without and with 10 mM BTA. At this BTA concentration no effect of further addition of BTA was observed on cyclic voltammetry, H isotherm measure-

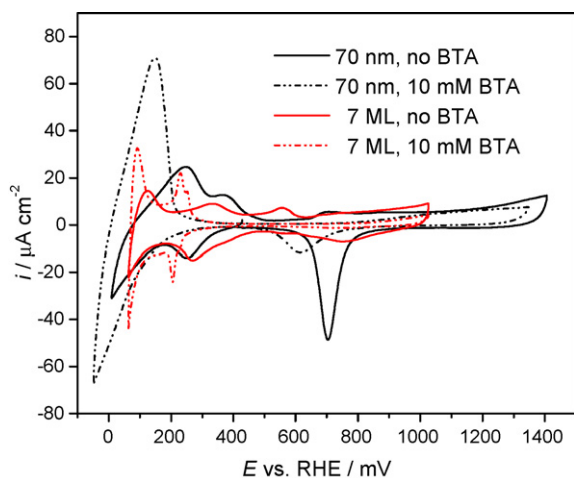


Fig. 8. Cyclic voltammograms at 70 nm Pd/Au(polycrystal) and 7 ML Pd/Au(111) deposit, in 0.1 M NaOH (—) and 0.1 M NaOH + 10 mM BTA (---); scan rate: 10 mV s^{-1} .

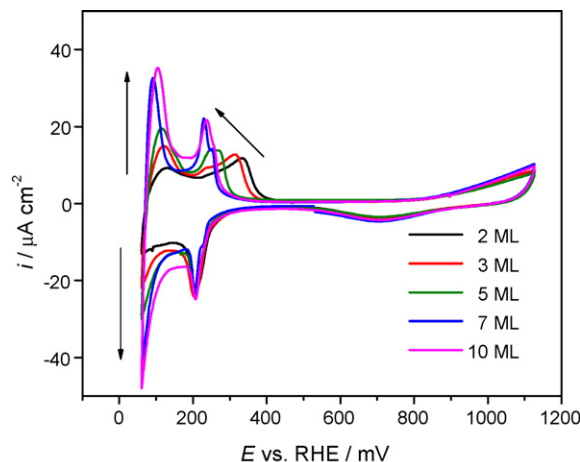


Fig. 9. Cyclic voltammograms at 2–10 ML Pd/Au(111) deposit, in 0.1 M NaOH + 10 mM BTA; scan rate: 10 mV s^{-1} .

ments and impedance spectroscopy. It was concluded that the surface was saturated by BTA at 10 mM. The protective effect in the oxidation potential range, i.e. at potentials more positive than 500 mV, is clearly visible at both deposits. At potentials lower than 500 mV, adsorption is at least partially inhibited while absorption is promoted.

At 70 nm Pd/Au(polycrystal) only large absorption/desorption peaks are visible in the presence of BTA. They are shifted to more negative potentials and are more reversible than those observed in the absence of BTA. However, at thin layers of Pd/Au(111) a new sharp pair of peaks around 250 mV appears on the cyclic voltammograms followed, at more negative potentials, by a pair of peaks due to H adsorption/desorption. The main effect responsible for the absorption promotion observed on cyclic voltammograms (peaks at more negative potentials) is kinetic since the increase in the absorption/desorption reaction reversibility is very important. This is confirmed by impedance measurements (see later).

Fig. 9 displays voltammograms at 2–10 ML Pd/Au(111) in NaOH + BTA. The thickness dependence of the H absorption current below 150 mV is as expected, i.e. it increases with the thickness. More interesting is the analysis of the cathodic and anodic peaks around 250 mV. The cathodic peak is totally independent of the thickness, suggesting that it represents a surface phenomenon. This suggests a change in the BTA layer, which would start at 280 mV (foot of the peak). BTA total desorption is improbable because an effect on H adsorption at more negative potentials can also be seen. More probable is a reorientation of the BTA layer at the Pd surface followed by hydrogen adsorption. BTA reorientation was already observed on copper in the Cu oxidation potential range using FTIR and STM [58,59]. The behavior of the anodic peak is more unusual. The position and the shape of the peak, and thus the reversibility of the reaction, strongly depend on the thickness up to 5 ML, increasing with the Pd layer thickness. Substrate effects can be pointed as the main reason for this effect. It should be added that in sulfuric acid a shift of hydrogen adsorption peaks into positive direction upon addition of BTA was also observed [22] with the final voltammogram similar to that observed in NaOH.

EIS can provide interesting data to confirm the hypothesis of a modification in the BTA layer. However, classical stationary impedance was not adequate to confirm the kinetic difference between the adsorption and desorption peaks. Thus, we completed our study with dynamic electrochemical impedance spectroscopy (DEIS) where sum of sinusoidal perturbations was applied during the potential sweep followed by the FFT analysis of the potential and current signals to obtain the impedance spectra during the sweep and from the modeling of the impedance data the charge transfer

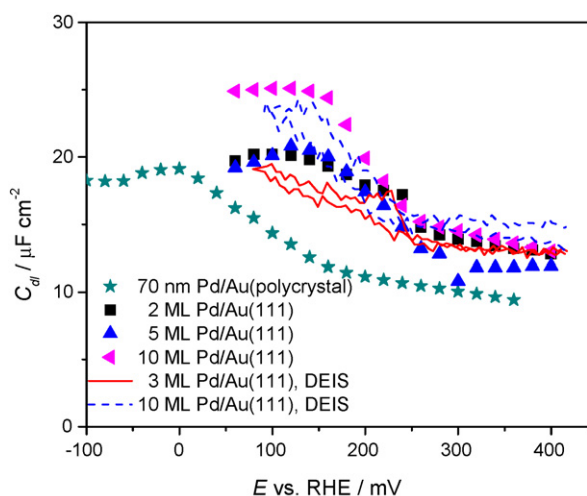


Fig. 10. Double layer capacitance C_{dl} at 70 nm Pd/Au(polycrystal) and 2–10 ML Pd/Au(111) deposit, in 0.1 M NaOH + 10 mM BTA obtained using stationary and dynamic (DEIS) electrochemical impedance spectroscopy.

resistance and the double layer capacitance. The equivalent circuit used to fit our results was the same as described above. Since BTA also protects Pd from contamination, it was possible to work at lower frequencies and observe the low frequency capacitive behavior. However, the used sweep rate was 2 mV s^{-1} what limited the lowest frequency at 2 Hz.

Fig. 10 displays the potential dependence of the average double layer capacitance at 70 nm Pd/Au(polycrystal) film and at 2–10 monolayers at Au(111) in NaOH with BTA. It clearly exhibits the typical C_{dl} potential evolution characteristic for the specific adsorption of an organic molecule at the Pd surface with both techniques. This adsorption decreases the double layer capacitance at the most positive potentials. Below 180 mV at the 70 nm Pd film and 280 mV at Pd monolayers, C_{dl} slowly increases until reaching a value around $20 \mu\text{F cm}^{-2}$. This value is similar to what was obtained without BTA at negative potentials. Moreover, the increase starts at potentials where the cathodic peak is observed at monolayers in Fig. 9. This is relevant to the hypothesis of a change in the BTA layer orientation. However, a sharp peak in C_{dl} is expected for such a phenomenon. This peak cannot be seen when focusing on the average C_{dl} , Fig. 10. The parallel observation of T and ϕ parameters at Pd/Au(111) monolayers gives more information in Fig. 11. The dependence of T parameter displays the expected peak at the potentials corresponding to the voltammetric peak. At the same potential, ϕ strongly decreased. This diminution of ϕ compensates the increase of T in the calculation of C_{dl} , see equation above. This explains why no peak is observed in Fig. 10. The obtained data suggest that analysis of the CPE parameters T and ϕ instead of the average C_{dl} is more sensitive in the case of specific adsorption. The peaks are observed with the stationary EIS and DEIS. However, DEIS presents two peaks: a small one corresponding to the cathodic part of the voltammogram (potentials decreasing from 420 to 80 mV), and an intense one for the anodic part (potentials increasing from 80 to 420 mV). These peaks perfectly match with those observed in Fig. 9. The peak observed with EIS seems to be the mean of the two peaks obtained by DEIS.

Fig. 12 presents the potential dependence of the charge transfer resistance R_{ct} and the low frequency capacitance C_{LF} at 70 nm Pd/Au(polycrystal) 2–10 ML Pd/Au(111) deposits, in 0.1 M NaOH + 10 mM BTA. By comparing Fig. 7 and Fig. 12, it is clear that BTA decreased R_{ct} by more than one order of magnitude, and thus can be considered as a kinetic promoter for H sorption. Such effect was also observed with other poisons and electrode materi-

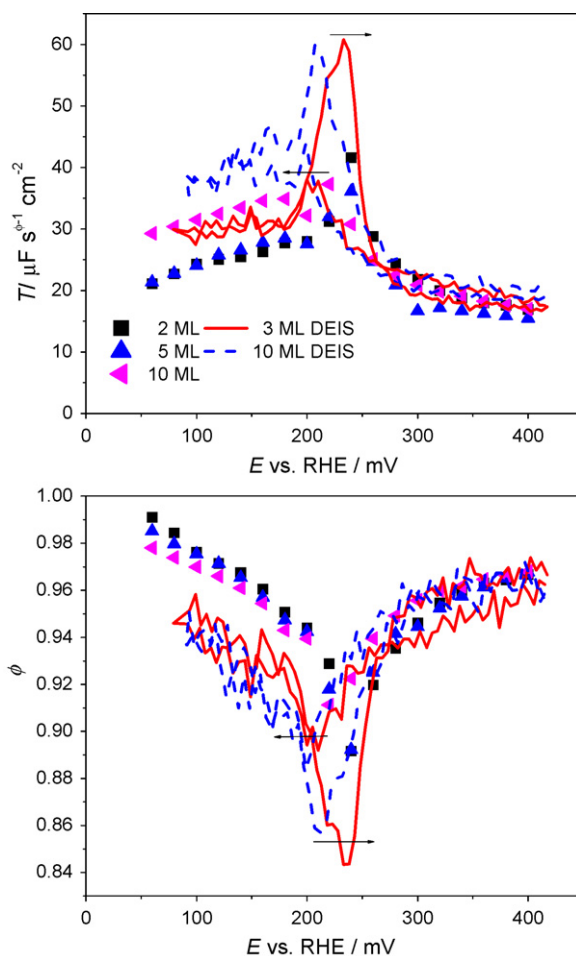


Fig. 11. T and ϕ parameters obtained by EIS and DEIS, at 2–10 ML Pd/Au(111), in 0.1 M NaOH + 10 mM BTA. The arrows indicate the direction of the potential sweep in DEIS.

als [13,29,31]. BTA addition strongly decreases the influence of the thickness on R_{ct} since no clear tendency was observed at Pd monolayers and nanometric films, and the values of R_{ct} for both types of deposits are of the same order of magnitude. R_{ct} values obtained from DEIS experiments at 3 ML Pd exhibit an important difference between adsorption and desorption reactions. The difference between the forward (decreasing potentials) and the backward (increasing potentials) runs is important at this deposit, while both are quite similar at 10 ML. This confirms what was observed with cyclic voltammetry in Fig. 9. In parallel with R_{ct} is shown the C_{LF} potential dependence. C_{LF} at Pd monolayers exhibits two distinctive domains: above 240 mV, H adsorption is mainly blocked by BTA; below 240 mV, H adsorption can be achieved since a change in the adsorbed BTA layer occurs (see voltammograms in Fig. 9 and double layer capacitance parameters in Fig. 11). A peak of C_{LF} at 250 mV is also visible suggesting hydrogen adsorption.

Fig. 13 displays the total H sorption isotherms and the contributions of individual processes at 30 nm Pd deposit in 0.1 M NaOH with and without 10 mM BTA. In our previous work on Pd deposits in NaOH [18], contributions to the adsorption and absorption were estimated at this Pd film. The comparison between the isotherm with BTA and the adsorbed H charge suggests that BTA blocks H adsorption. However, the H charge in the presence of BTA is larger than that due to H absorption only. That confirms that BTA inhibits H adsorption only partially.

In Fig. 14, the influence of BTA on H adsorption and absorption at 2, 5 and 10 Pd ML is demonstrated. The effect on ultra thin deposits

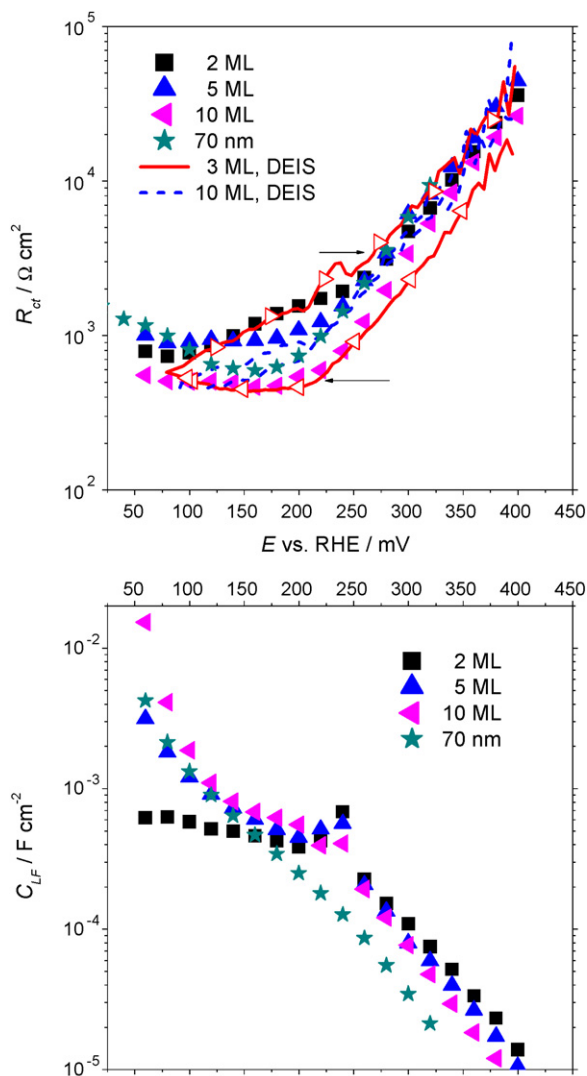


Fig. 12. Charge transfer resistance R_{ct} and low frequency capacitance C_{LF} at 70 nm Pd/Au(polycrystal) deposit, and 2–10 ML Pd/Au(111) deposits, in 0.1 M NaOH + 10 mM BTA. The arrows indicate the direction of the potential sweep in DEIS.

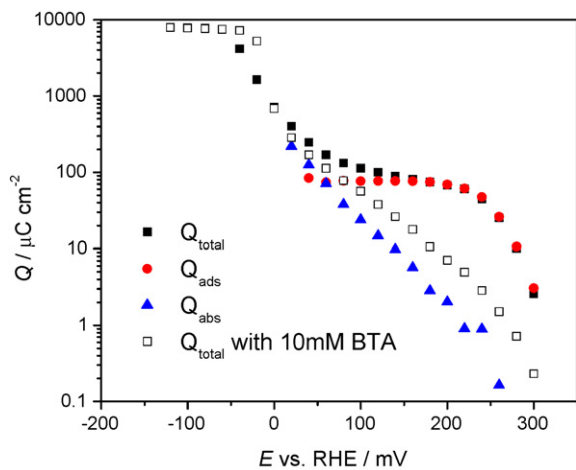


Fig. 13. H sorption isotherms at a 30 nm Pd/Au(polycrystal) deposit, with a real surface area of 0.79 cm²; total H charge (■), adsorbed H charge (●), absorbed H charge (▲) in 0.1 M NaOH, total H charge in 0.1 M NaOH + 10 mM BTA (□).

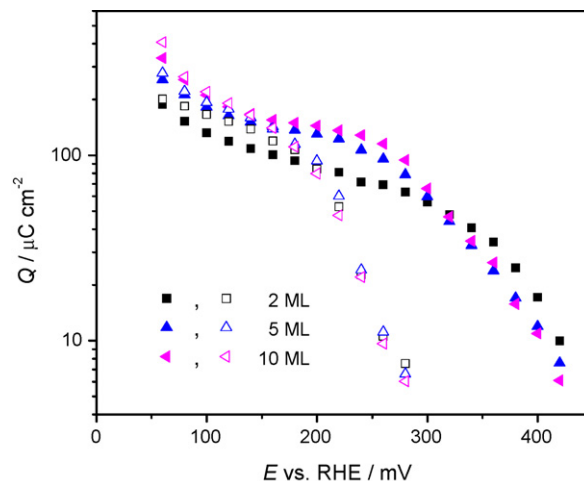


Fig. 14. Total H sorption charge at 2 ML (■), 5 ML (▲) and 10 ML (▼) Pd/Au(111) deposits, in 0.1 M NaOH (filled symbols) and 0.1 M NaOH + 10 mM BTA (open symbols).

is similar to what is observed at nanometric films, Fig. 13. Since no influence of the thickness can be observed at 2–10 ML Pd/Au(111) deposits in NaOH + BTA between 240 and 280 mV, the hypothesis of residual adsorption seems to be confirmed. Once more, 240 mV seems to be a transition point, suggesting a rearrangement of the BTA layer.

Results shown in Figs. 13 and 14 indicate that BTA inhibits partially hydrogen adsorption but does not affect hydrogen absorption into metal. This behavior is similar to that found in acid solutions in the presence of another poison, crystal violet [13,14]. These results clearly indicate that hydrogen absorption in the presence of poisons must proceed through the direct mechanism. In the case of the indirect mechanism hydrogen adsorption and absorption are related according to: $\mu_{H,ads} = \mu_{H,abs}$, that is the chemical potential of adsorbed hydrogen equals to that of absorbed one and decrease of the surface coverage by adsorbed hydrogen leads to decrease of $\mu_{H,ads}$ and decrease of the quantity of absorbed hydrogen, what is not experimentally observed.

4. Conclusions

Hydrogen adsorption and absorption at Pd monolayers deposited on Au(111) have been studied in the absence and in the presence of benzotriazole. The following conclusions can be drawn:

1. H adsorption at Pd/Au(111) monolayers starts at more positive potentials than at nanometric Pd/Au(polycrystal) films.
2. H adsorption and absorption at Pd/Au(111) monolayers are more reversible than at nanometric Pd/Au(polycrystal) films.
3. These two observations are a consequence of the strong substrate influence due to geometric and electronic effects.
4. BTA blocks partially adsorption and promotes kinetically absorption.
5. There is a modification in the adsorbed BTA layer orientation around 240 mV at Pd/Au(111) monolayers.
6. Gold substrate also influences H sorption at Pd monolayers in NaOH + BTA up to 5 monolayers.
7. The results obtained in the presence of poison point out to the direct H absorption mechanism.

Acknowledgements

Financial support from CRSNG (Canada) is gratefully acknowledged.

The authors acknowledge Prof. D. Harrington (University of Victoria) for supplying the program for data acquisition/analysis and Daniel Auger (Université de Sherbrooke) for constructing the electronics for DEIS.

References

- [1] F.A. Lewis, *The Palladium Hydrogen Systems*, Academic Press, London, 1967.
- [2] G. Alefeld, J. Völkl (Eds.), *Hydrogen in Metals*, vols. I and II, Springer-Verlag, Berlin, 1978.
- [3] M. Baldauf, D.M. Kolb, *J. Phys. Chem.* 100 (1996) 11375.
- [4] S. Pandelov, U. Stimming, *Electrochim. Acta* 52 (2007) 5548.
- [5] A. Czerwinski, *Electrochim. Acta* 39 (1994) 431.
- [6] A. Czerwinski, R. Marassi, *J. Electroanal. Chem.* 322 (1992) 373.
- [7] A. Czerwinski, R. Marassi, S. Zamponi, *J. Electroanal. Chem.* 316 (1991) 211.
- [8] A. Czerwinski, *Polish. J. Chem.* 69 (1995) 699.
- [9] A. Czerwinski, G. Maruszczak, M. Zelazowska, M. Lancucka, R. Marassi, S. Zamponi, *J. Electroanal. Chem.* 386 (1995) 207.
- [10] A. Czerwinski, M. Czauderna, G. Maruszczak, I. Kiersztyn, R. Marassi, S. Zamponi, *Electrochim. Acta* 42 (1997) 81.
- [11] A. Czerwinski, I. Kiersztyn, M. Grden, J. Czapla, *J. Electroanal. Chem.* 471 (1999) 190.
- [12] A. Czerwinski, I. Kiersztyn, M.S. Grden, *J. Electroanal. Chem.* 492 (2000) 128.
- [13] L. Birry, A. Lasia, *Electrochim. Acta* 51 (2006) 3356.
- [14] H. Duncan, A. Lasia, *Electrochim. Acta* 53 (2008) 6845.
- [15] C. Gabrielli, P.P. Grand, A. Lasia, H. Perrot, *J. Electrochem. Soc.* 151 (2004) A1937.
- [16] C. Gabrielli, P.P. Grand, A. Lasia, H. Perrot, *J. Electrochem. Soc.* 151 (2004) A1943.
- [17] C. Gabrielli, P.P. Grand, A. Lasia, H. Perrot, *J. Electrochem. Soc.* 151 (2004) A1925.
- [18] M.H. Martin, A. Lasia, *Electrochim. Acta* 53 (2008) 6317.
- [19] J. Paillier, L. Roué, *J. Electrochem. Soc.* 152 (2005) E1.
- [20] J. Clavilier, J.-P. Gnanon, M. Petit, *J. Electroanal. Chem.* 265 (1989) 231.
- [21] G.A. Attard, A. Bannister, *J. Electroanal. Chem.* 300 (1991) 467.
- [22] M. Baldauf, D.M. Kolb, *Electrochim. Acta* 38 (1993) 2145.
- [23] L.A. Kibler, A.M. El-Aziz, D.M. Kolb, *J. Mol. Catal. A: Chem.* 199 (2003) 57.
- [24] L.A. Kibler, M. Kleinert, R. Randler, D.M. Kolb, *Surf. Sci.* 443 (1999) 19.
- [25] J. Tang, M. Petri, L.A. Kibler, D.M. Kolb, *Electrochim. Acta* 51 (2005) 125.
- [26] R. Hoyer, L.A. Kibler, D.M. Kolb, *Electrochim. Acta* 49 (2003) 63.
- [27] L.A. Kibler, A.M. El-Aziz, R. Hoyer, D.M. Kolb, *Ang. Chem. Int. Ed.* 44 (2005) 2080.
- [28] R. Hoyer, L.A. Kibler, D.M. Kolb, *Surf. Sci.* 562 (2004) 275.
- [29] H. Duncan, A. Lasia, *Electrochim. Acta* 52 (2007) 6195.
- [30] H. Duncan, A. Lasia, *J. Electroanal. Chem.* 621 (2008) 62.
- [31] B.E. Conway, J.H. Barber, L. Gao, S.Y. Qian, *J. Alloys Compd.* 253–254 (1997) 475.
- [32] S.Y. Qian, B.E. Conway, G. Jerkiewicz, *J. Chem. Soc., Farad. Trans.* 94 (1998) 2945.
- [33] L. Birry, Ph.D. Thesis, Université de Sherbrooke, 2005.
- [34] J.N. Han, S.I. Pyun, T.H. Yang, *J. Electrochem. Soc.* 144 (1997) 4266.
- [35] M.W. Breiter, *J. Electroanal. Chem.* 109 (1980) 243.
- [36] M.W. Breiter, *J. Electroanal. Chem.* 109 (1980) 253.
- [37] M.W. Breiter, *J. Electroanal. Chem.* 180 (1984) 25.
- [38] A. Czerwinski, *J. Electroanal. Chem.* 379 (1994) 487.
- [39] A. Czerwinski, S. Zamponi, R. Marassi, *J. Electroanal. Chem.* 304 (1991) 233.
- [40] B. Łosiewicz, L. Birry, A. Lasia, *J. Electroanal. Chem.* 611 (2007) 26.
- [41] P.N. Bartlett, B. Gollas, S. Guerin, J. Marwan, *Phys. Chem. Chem. Phys.* 4 (2002) 3835.
- [42] P.N. Bartlett, J. Marwan, *Phys. Chem. Chem. Phys.* 6 (2004) 2895.
- [43] M.H.A. Elhamid, B.G. Ateya, H.W. Pickering, *J. Electrochem. Soc.* 144 (1997) L58.
- [44] N. Amokrane, C. Gabrielli, G. Maurin, L. Mirkova, *Electrochim. Acta* 53 (2007) 1962.
- [45] S. Szpak, P.A. Mosier-Boss, S.R. Scharber, J.J. Smith, *J. Electroanal. Chem.* 337 (1992) 147.
- [46] A. Hamelin, B.E. Conway, J.O'M. Bockris, in: R.E. White (Ed.), *Modern Aspects of Electrochemistry*, vol. 16, Kluwer/Plenum, New York, 1985, p. 1.
- [47] D.F. Yang, C.P. Wilde, M. Morin, *Langmuir* 12 (1996) 6570.
- [48] G.S. Popkurov, R.N. Schindler, *Rev. Sci. Instr.* 64 (1993) 3111.
- [49] A.E. Bolzan, *J. Electroanal. Chem.* 380 (1995) 127.
- [50] G. Denuault, C. Milhano, D. Pletcher, *Phys. Chem. Chem. Phys.* 7 (2005) 3545.
- [51] A.M. El-Aziz, R. Hoyer, L.A. Kibler, D.M. Kolb, *Electrochim. Acta* 51 (2006) 2518.
- [52] A. Sellidj, B.E. Koel, *Phys. Rev. B* 49 (1994) 8367.
- [53] B. Hammer, J.K. Nørskov, *Surf. Sci.* 343 (1995) 211.
- [54] A. Ruban, B. Hammer, P. Stolze, H.L. Skriver, J.K. Nørskov, *J. Mol. Catal. A* 115 (1997) 421.
- [55] C. Lebouin, Ph.D. Thesis, INP Grenoble, 2008.
- [56] G.J. Brug, A.L.G. van den Eeden, M. Sluyters-Rehbach, J.H. Sluyters, *J. Electroanal. Chem.* 176 (1984) 275.
- [57] A. Lasia, B.E. Conway, J.O'M. Bockris, in: R.E. White (Ed.), *Modern Aspects of Electrochemistry*, vol. 32, Kluwer/Plenum, New York, 2002, p. 143.
- [58] M.R. Vogt, R.J. Nichols, O.M. Magnussen, R.J. Behm, *J. Phys. Chem. B* 102 (1998) 5859.
- [59] Z.D. Schultz, M.E. Biggin, J.O. White, A.A. Gewirth, *Anal. Chem.* 76 (2004) 604.